

Propagation of a Gaussian-Schell Model Beam Array Through Atmospheric Turbulence in a Slanted Path

T.G. ZHAO*, Z.H. YANG AND G.H. WU

*School of Electronic Engineering, Beijing University of Posts and Telecommunications,
Beijing 100876, China*

A one-dimensional (1-D) beam array consists of off-axis Gaussian-Schell model (GSM) beams is studied. Based on the extended Huygens-Fresnel principle, the analytical expressions for the average intensity, the mean-squared beam width and the far-field angular spread of the GSM beam array propagating through atmospheric turbulence in a slanted path are derived. Results show that the beam width broadening can be improved by choosing a proper optical wavelength, initial waist width and correlation length of the source. With the increasing number of the individual beams which compose the array, the far-field angular spread will increase. The conclusion is exact the opposite when the propagation happened in free space atmosphere.

Keywords: Laser beam, beam array, turbulence, slanted path, Gaussian-Schell model (GSM), Huygens-Fresnel principle, far-field angular spread

1 INTRODUCTION

Due to the advantages like low cost, high directionality and high-rate data capacity, the propagation of laser beams through atmospheric turbulence has attracted considerable attention recently, which is an important subject for many applications, such as remote sensing, imaging and tracking [1–4]. But during the propagation, the laser beams will be greatly affected by turbulence, which will cause intensity fluctuations, intensity fading, additional

*Corresponding author: E-mail: zhaotg@bupt.edu.cn

beam spreading, etc., directly affecting the quality and stability of the propagation [5]. Clearly, the study on this subject has been attached with great practical significance and urgency. Much work that concerns the propagation properties of the laser beams through atmospheric turbulence has been carried out so far [6–11]; however, most of these studies have been restrained to the cases of the horizontal path [12–13], while the slanted path is more important and more promising in many applications, such as deep-space and ground-satellite optical communications [14].

The case of the slanted path is taken as the study object in this paper. Since partially coherent beams are less sensitive to the effects of turbulence [15] and the beam combination [16] is a good way to achieve high system powers, a one-dimensional beam array consisting of M individual off-axis Gaussian Schell (GSM) model beams is selected as the light source.

Based on the extended Huygens-Fresnel principle, the analytical expression for the received intensity [17], the mean-squared beam width [18] and the far-field angular spread [19] in a slanted path are derived.

2 PROPAGATION EQUATION

We assume in Figure 1 that a one-dimensional (1-D) beam array in rectangular symmetry consists of M individual off-axis Gaussian Schell (GSM) model beams positioned at the plane $z = 0$ whose separate distance is set to x_d . It is obvious that the nature of the source determines how the beam behaves [20]. In this paper, the M individual sources are assumed to be uncorrelated. The cross-spectral density function of the individual beam, $W^{(0)}$, can be expressed as

$$W^{(0)}(x_1', x_2', 0) = \exp \left[\frac{(x_1' - mx_d)^2 + (x_2' - mx_d)^2}{w_0^2} \right] \exp \left[-\frac{(x_1' - x_2')^2}{2\sigma_0^2} \right] \quad (1)$$

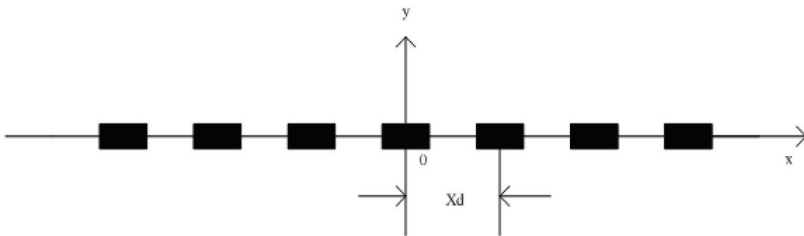


FIGURE 1
Sketch of the beam array in rectangular coordinate system.

where w_0 is the original beam waist width, σ_0 is the correlation length and $m \in \left[-\frac{m-1}{2}, \frac{m+1}{2} \right]$.

In order to simplify the calculation, M is considered as an odd number and we set the centre of the beams at the point of $(mx_d, 0)$. As the M individual GSM beams are uncorrelated, the superposition of the intensity at the plane $z = 0$ is derived:

$$I(x, z = 0) = \sum_{m=\frac{M-1}{2}}^{\frac{M+1}{2}} \exp \left[-\frac{2(x - mx_d)^2}{w_0^2} \right] \tag{2}$$

Based on the extended Huygens-Fresnel principle, the cross-spectral density function of the GSM beams at the plane of $z = L$ can be expressed as

$$W^{(0)}(x_1, x_2, L) = \frac{1}{\lambda L} \iint dx_1 dx_2 W^{(0)}(x_1, x_2, 0) \exp \left[-ik \frac{(x_1' - x_1)^2 - (x_2' - x_2)^2}{2L} \right] \tag{3}$$

$$\left\{ \exp \left[\psi^*(x_1', x_1) + \psi(x_1', x_1) \right] \right\}_m$$

where k is the wave number associated with the frequency ω or related to the wavelength λ , L is the propagation distance of the slanted path and the subscript m denotes the average over the ensemble of the turbulent medium [21]:

$$\left\{ \exp \left[\psi^*(x_1', x_1) + \psi(x_1', x_1) \right] \right\}_m = \exp \left[05D_\psi(x_1' - x_2', x_1 - x_2) \right] \tag{4a}$$

or

$$\left\{ \exp \left[\psi^*(x_1', x_1) + \psi(x_1', x_1) \right] \right\}_m$$

$$\cong \exp \left[-\frac{(x_1' - x_2')^2 + (x_1' - x_2')(x_1 - x_2) + (x_1 - x_2)^2}{\rho_0^2} \right] \tag{4b}$$

where $D_\psi(x_1' - x_2', x_1 - x_2)$ is the Rytov's phase structure function [22], $\psi(x', x)$ is the random part of the complex phase which denotes the atmospheric turbulence effects on the spherical waves and ρ_0 is the spatial coherence radius of a spherical wave and can be expressed as

$$\rho_0 = \left(0.545 \tilde{C}_n^2 k^2 L\right)^{-3/5} \quad (5)$$

with

$$\tilde{C}_n^2 = \frac{1}{H} \int_0^H C_n^2(h) dh \quad (6)$$

where C_n^2 is the altitude-dependent structure constant, h is the altitude from the ground and H is assumed as the altitude between the source plane and the receiver. Now, ξ denotes the zenith angle, and therefore L can be expressed as

$$L = H \sec \zeta \quad (7a)$$

and z can be expressed as

$$z = h \sec \zeta \quad (7b)$$

Radio communication sector of the International Telecommunication Union (ITU-R) describes the altitude-dependent structure constant like this [23]:

$$\begin{aligned} C_n^2(h) = & 8.1484 \times 10^6 V^2 h^{10} \exp\left(\frac{-h}{1000}\right) + 2.7 \times 10^{-16} \exp\left(\frac{-h}{1500}\right) \\ & + C_0 \exp\left(\frac{-h}{100}\right) \end{aligned} \quad (8)$$

where $V = (v_g^2 + 30.69v_g + 348.91)^{1/2}$ denoting the wind speed along the vertical path and v_g denotes the ground wind speed. The typical value of C_0 is $1.7 \times 10^{-14} \text{m}^{-2/3}$. For convenience, we set $v_g = 0$ in this paper.

The $W^{(0)}$ of the beam at the plane of $z = 0$ is expressed in Equation (1). Using the integral formula we can obtain

$$\int_{-\infty}^{\infty} \exp(-\beta^2 x + yx) dx = \frac{\sqrt{\pi}}{\beta} \exp\left(\frac{\gamma^2}{4\beta^2}\right) \quad (9)$$

Upon substituting Equation (1) into Equation (3) and letting $x_1 = x_2 = x$, we obtain the intensity expression of the GSM beams through atmospheric turbulence, I_m , after tedious integral calculations:

$$I_m(x, z) = W_m(x, x, z) \quad (10a)$$

or

$$I_m(x, z) = \frac{\varepsilon}{2\beta} \exp \left[-\frac{\varepsilon^2}{2\beta^2} \left(\frac{x}{w_0} - \frac{mxd}{w_0} \right)^2 \right] \quad (10b)$$

where

$$\beta = \sqrt{\frac{1}{w_0^4} + \frac{2}{w_0^2 \rho_0^2} + \frac{1}{w_0^4 \alpha^2} + \frac{\varepsilon^2}{4}} \quad (11a)$$

$$\varepsilon = \frac{k}{z} \quad (11b)$$

and

$$\alpha = \frac{\sigma_0}{w_0} \quad (11c)$$

with α being the coherence parameter. The superposition of the intensity turns out to be

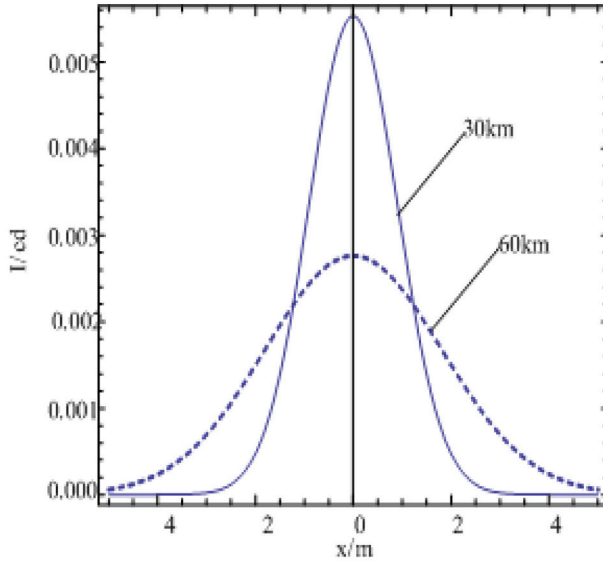
$$I_m(x, z) = \sum_{m=-\frac{M-1}{2}}^{\frac{M-1}{2}} I_m(x, z) \quad (12a)$$

or

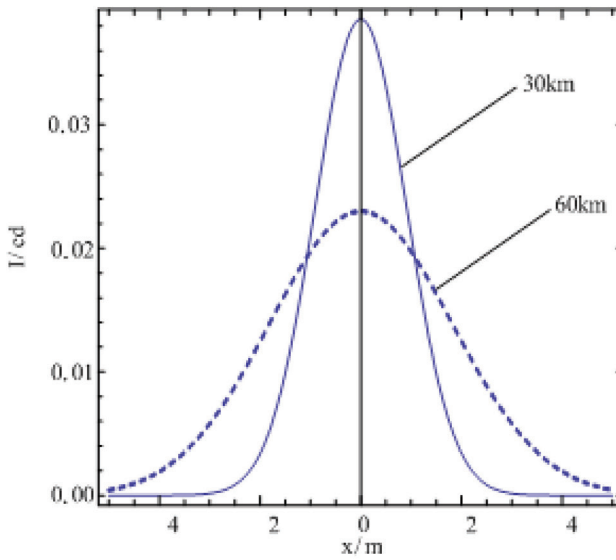
$$I_m(x, z) = \frac{\varepsilon}{2\beta} \sum_{m=-\frac{M-1}{2}}^{\frac{M-1}{2}} \exp \left[-\frac{\varepsilon^2}{2\beta^2} \left(\frac{x}{w_0} - \frac{mxd}{w_0} \right)^2 \right] \quad (12b)$$

From Equation (12a) and Equation (12b) we can see that the intensity distribution of the beams depends on the refraction index structure constant C_n^2 , separation distance x_d , propagation distance z and beam numbers M .

In this section we will use software to illustrate the propagation of the beams through atmospheric turbulence. Here $\lambda = 1550$ nm, $w_0 = 0.03$ m, $\sigma_0 = 0.03$ m, $x_d = 0.04$ m, $C_0 = 1.7 \times 10^{-14}$ and $\xi = \pi/3$. When the multiple beams are uncorrelated, the intensity can be obtained by the superposition of the intensity of the M individual beams [22]. Figure 2 shows the average intensity distribution of GSM beams through turbulence for different M value.



(a)



(b)

FIGURE 2

Graphs showing the intensity distribution of the beams with sources uncorrelated for (a) $M=1$ and (b) $M=7$ for propagation distances of $z=30$ km and $z=60$ km.

From Figure 2(a), it is obvious that the intensity is a Gaussian like profile in turbulence in this situation. The propagation altitude is set to 15 and 30 km with the zenith angle of $\xi = \pi/3$; that is, the propagation distance z is 30 and 60 km.

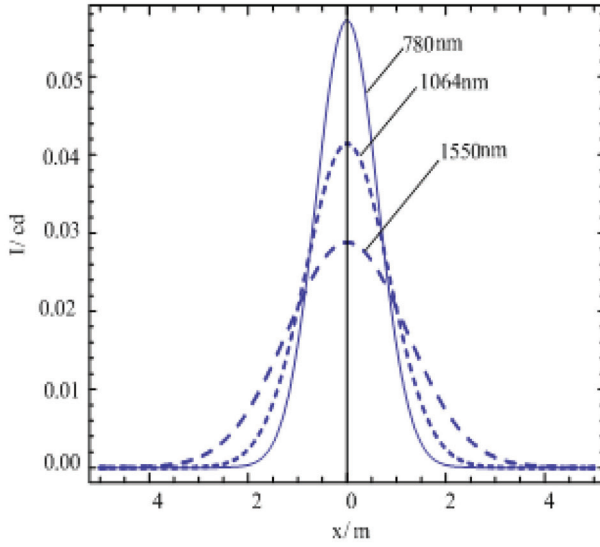
In Figure 2(a), the value of M is set to 1, which means the single beam case is taken into consideration. From the curve we see that the intensity decreases with the increasing propagation distance z . When propagation distance z increases from 30 to 60 km, the curve indicates that the beams have been expanded obviously as the peak value decreases. Figure 2(b) gives the intensity distribution of the multiple beams case when M is set to 7. By comparison, the curve in Figure 2(b) is similar to the one in Figure 2(a). After 30 km propagation, the peak value of the dashed curve reduces to almost half of the maximum in Figure 2(a) and Figure 2(b). If we keep on increasing the M value, the ratio will increase.

This means if we change the number of the individual beams, the far-field intensity distribution will be influenced. The greater the M value is, the smaller the loss of the optic signal attenuation is proportionately. When M increases to a certain value, the loss proportion will reach an upper limit. If certain value is exceeded, the loss ratio will reach a threshold, which will not be changed any more. Depending on the parameter settings in this case, the certain M value is 27.

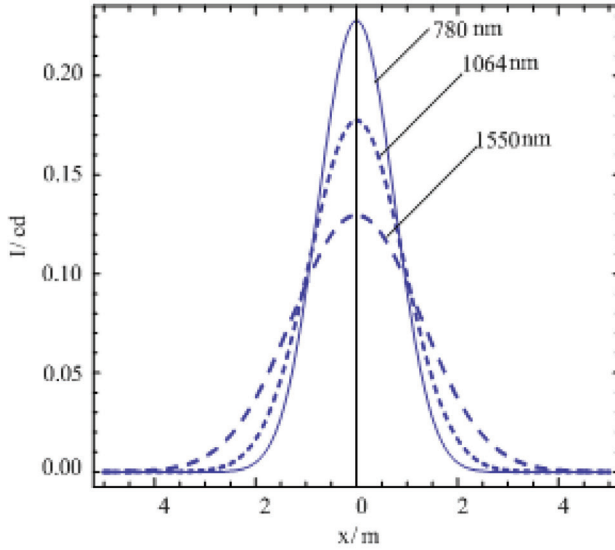
In Figure 3, we plot the intensity profiles of the beams with different wavelengths at $h = 40$ km. The calculation parameters are $w_0 = 0.02$ m, $\sigma_0 = 0.01$ m and $\xi = \pi/3$. The other parameters are the same as those of Figure 2. As indicated in Figure 3, the peak value of the average intensity decreases with the increasing wavelength. In contrast, the full width at half maximum (FWHM) of the curve increases with the increasing wavelength. In Figure 3(b), the differences between the three curves become smaller when compared to Figure 3(a), which means that the 1-D beam array can reduce the effect of wavelength changes to the intensity distribution.

When $\lambda = 1550$ nm and $M = 7$, the altitude is set to 40 km. While other parameters are the same as those of Figure 3, we change the value of the beam waist width to achieve Figure 4. From Figure 4 below, we can see that the parameter w_0 of the source greatly determines how the beam behaves. When the original beam waist width is $w_0 = 0.01$, $w_0 = 0.03$ and $w_0 = 0.06$ m the average intensity will increase with the increasing beam waist width. Selecting the appropriate beam waist width value can help us get the intensity we need. And Figure 4 indicates that, with the increasing beam waist width, the energy of the laser beams is relatively more concentrated.

In Figure 5 we plot the intensity profiles of the beams with different zenith angles. The angles are $\xi = 0$, $\xi = \pi/6$ and $\xi = \pi/4$. The other calculation parameters are the same as those of Figure 3. As can be seen, the average intensity decreases with increasing zenith angle. The reason is that as the



(a)



(b)

FIGURE 3

Graphs showing the average intensity of the GSM beams through turbulence in a slanted path at an altitude of 40 km for different wavelengths of $\lambda = 780$ nm, $\lambda = 1064$ nm and $\lambda = 1550$ nm when (a) $M = 1$ and (b) $M = 7$.

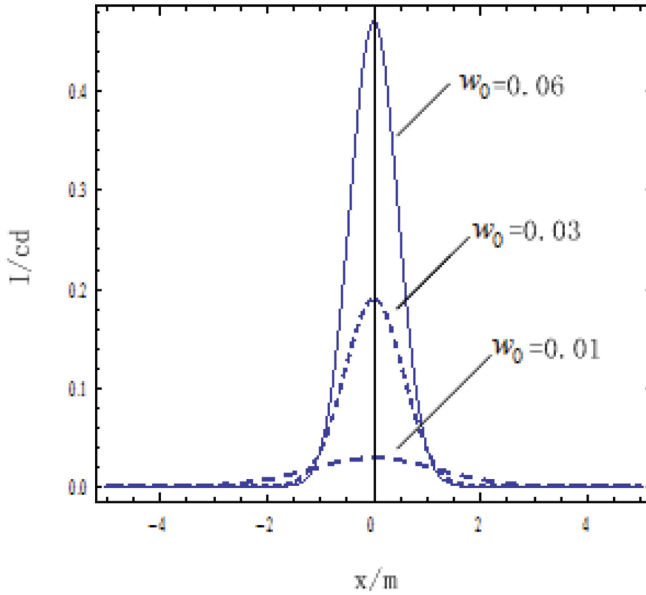


FIGURE 4
Graph showing the average intensity of the GSM beams through atmospheric turbulence in a slanted path for different initial beam waists of $w_0 = 0.06$ m, $w_0 = 0.03$ m and $w_0 = 0.01$ m.

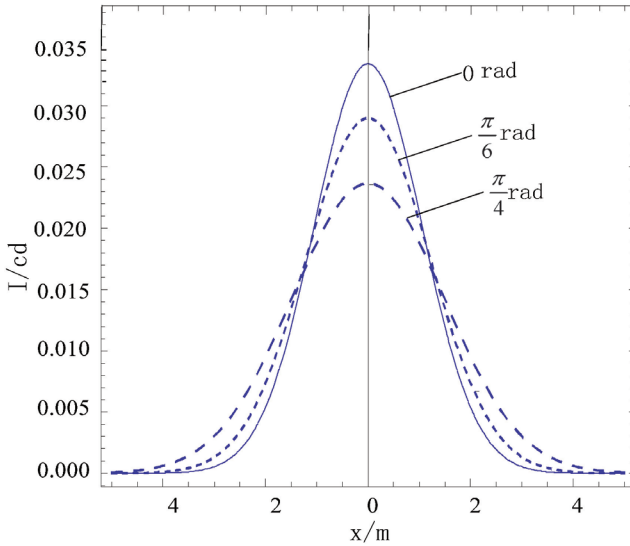


FIGURE 5
Graph showing the average intensity of the GSM beams through atmospheric turbulence in a slanted path for different zenith angles at the altitude of 40 km, where the zenith angle is $\xi = 0$, $\xi = \pi/6$ and $\xi = \pi/4$.

zenith angle increases while the altitude keep invariable, the propagation distance increased equivalently. With longer distance, the intensity will be more affected by turbulence.

3 MEAN-SQUARED BEAM WIDTH

The mean-squared beam width is always introduced as a basic physical quantity to describe the characteristics of the laser beam. It is defined as

$$w^2(x, z) = \frac{4 \int_{-\infty}^{\infty} x^2 I(x, L) dx}{\int_{-\infty}^{\infty} I(x, L) dx} \quad (13)$$

Upon substituting Equation (12b) into Equation (13) and performing integrations, we obtain

$$w^2(z) = \frac{4}{M} \sum_{m=-\frac{M-1}{2}}^{\frac{M-1}{2}} \left[\left(\frac{w_0 \beta}{2\varepsilon} \right)^2 + (mx_d)^2 \right] \quad (14)$$

The width of the beams propagating through turbulence when the distance between the source and the receiver increases is shown in Figure 6 for the superposition of the intensity, where we take $w_0 = 0.01$ m, $\sigma_0 = 0.03$ m, $x_d = 0.04$ m, $C_0 = 1.7 \times 10^{-14}$, $M = 5$ and $\xi = \pi/3$. Indicated in Figure 6, the solid curve denotes the beam width in turbulence (C_n^2 varies with the altitude gradually) and the dashed curve denotes the beam width in free space ($C_n^2 = 0$). We can see that the beam width broadened significantly as the distance increases, the solid curve grows faster than the dashed one.

Comparing the two situations we can conclude that it is only possible to change the wavelength parameter at a time while keeping the other parameters constant. In free space the broadening of the beam is very weak, which is almost independent of the wavelength. In turbulence, if the distance keeps increasing to 30 km, the curve will accelerate upward. For the same set of parameters, when the wavelength is set to 1064 nm, the broadening of the optical signal is more than the 1550 nm case, which means that the beam width broadening can be improved by choosing proper optical wavelength of the source. From the propagation altitude of 20 to 40 km, the beam width increases by almost 37%.

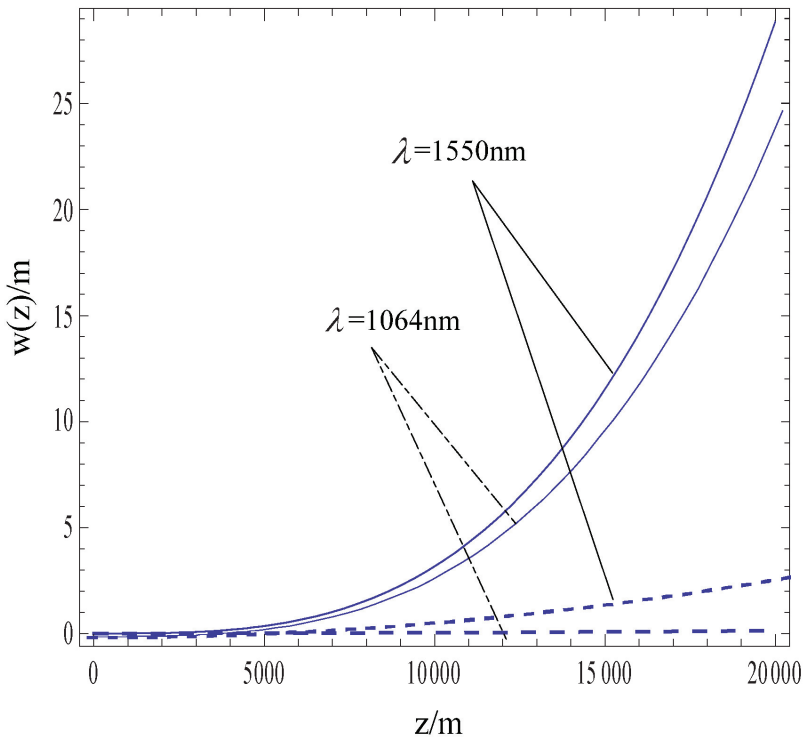


FIGURE 6

Graph showing the beam width of the GSM beams through atmospheric turbulence in a slanted path for $\lambda = 1550 \text{ nm}$ and $\lambda = 1064 \text{ nm}$ with $C_n^2 = 0$.

4 ANGULAR SPREAD OF THE GAUSSIAN-SCHELL MODEL (GSM) BEAMS IN TURBULENCE

In this part the far-field angular spread of GSM beams is studied. Beam directionality is chosen as the characteristic parameter [23]. The angular spread, θ_{sp} , of the GSM beams propagating through turbulence turns out to be [21]

$$\rightarrow \theta_{sp}(z) = \lim_{z \rightarrow \infty} \frac{\omega(z)}{z} \quad (15a)$$

or

$$\theta_{sp}(z) = \frac{2}{\sqrt{M}} \left[\sum_{m=-\frac{M-1}{2}}^{\frac{M-1}{2}} \left(\frac{\beta_0 w_0^2}{k^2} \right) \right]^{1/2} \quad (15b)$$

where

$$\beta_0 = \frac{1}{\omega_0^4} + \frac{2}{\omega_0^2 \rho^2} + \frac{1}{\omega_0^4 \alpha^2} \quad (16)$$

Upon substituting Equation (16) into Equation (15b) we obtain

$$\theta_{sp}(z) = \frac{2}{k\sqrt{M}} \left[\sum_{m=-\frac{M-1}{2}}^{\frac{M-1}{2}} \left(\frac{1}{\omega_0^4} + \frac{1}{\omega_0^4 \alpha^2} + F_z z^{6/5} \right) \right]^{1/2} \quad (17)$$

where

$$F_z = \frac{1.308}{\omega_0^2} \left(\tilde{C}_n^2 k^2 \right)^{6/5} \quad (18)$$

Now, θ_{sp} can also be expressed as

$$\theta_{sp}(z) = \frac{2}{k\sqrt{M}} \left[\sum_{m=-\frac{M-1}{2}}^{\frac{M-1}{2}} \left(\frac{1}{\omega_0^2} + \frac{1}{\sigma^2} + F_z' z^{6/5} \right) \right]^{1/2} \quad (19)$$

where

$$F_z = 1.308 \left(\tilde{C}_n^2 k^2 \right)^{6/5} \quad (20)$$

Equation (19) shows that the angular spread of the GSM beams is determined by beam parameters and the altitude-dependent structure constant. The first and the second term in Equation (19) represent the angular spread of GSM array beams in free space, which is dependent on the beam parameters. In the far-field, the influence of the beam parameters will be weakened, the F_z will dominate Equation (19) for the angular spread and F_z is independent of the coherence parameter.

The angular spread of the GSM beams *versus* the propagation distance z with different M value is shown in Figure 7. In free space, the far-field angular spread decreases with the increasing M value. While in turbulence, it shows that the angular spread rises with the increasing M value and the shape of the growth curve is similar to each other. The curve growth is fast in the initial period (0 to 10km), but slow in later period (10 to 30km). When z increases to 35 km, the curve flattens out and stops growing gradually. When

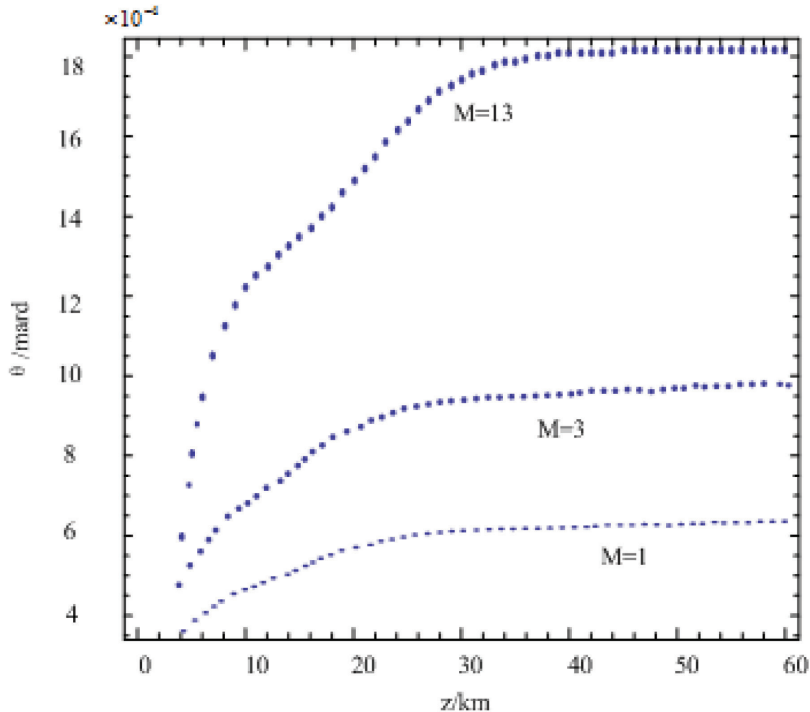


FIGURE 7

Graph showing the angular spread *versus* the propagation distance with different M values.

the curve is almost horizontal, the far-field divergence angle are depicted. This can be explained as follows. On the one hand, in the far-field, the value of the distance z is relatively large, but the altitude-dependent structure constant keeps on decreasing to a small value. Under this circumstance, the product of z and F_z will approach a steady value at one point. On the other hand, when the product is large enough to dominate the value of θ_{sp} , the value will hardly be affected by the first and second term in Equation (19). So the later part of the curve becomes flat when the steady point reaches.

Other cases are compared with the case of the single beam ($M = 1$) one by one. When $M = 3$, the angular spread is 2.236 times as much as the single beam case, and the number is 3.605 when $M = 13$ respectively. As it can be seen from the data, we know that with the increasing M value, the angular spread increases, but the increase rate is decreased by degrees.

The angular spread of the GSM beams *versus* the initial beam width is shown in Figure 7. The propagation distance is set to 10 km, the other calculation parameters are $M = 7$, $\sigma = 0.01$ m and $\lambda = 1550$ nm. From Equation (19) it is obvious that the angular spread decreases with the increasing the original beam waist. As indicated by Figure 7, the curve falls into two parts. The first

part dropping steeply when the original beam waist is smaller than 0.15 m and later part dropping slowly until the curve runs nearly parallel to the horizontal axis.

5 CONCLUSIONS

The propagation of an incoherent Gaussian-Schell model (GSM) beam array through atmospheric turbulence in a slanted path has been investigated. The average intensity, the mean-squared beam width and the angular spread of the beams are derived. It has been shown that the intensity is a Gaussian-like profile in turbulence and the loss of the optic signal attenuation will get smaller proportionately when the number of individual sources increases. By studying the parameters of the source we know that the parameters will greatly determine how the beam behaves and the beam width broadening can be improved by choosing a proper optical wavelength, initial waist width and correlation length of the source. As can be seen from the study of the far-field angular spread, we know that with the increasing the number of individual sources, the angular spread will increase, but the increase rate decreases by degrees. The conclusion is exact the opposite in free space situation.

NOMENCLATURE

C_n^2	Altitude-dependent structure constant
h	Altitude from the ground (km)
H	Assumed as the altitude between the source plane and the receiver (km)
I_m	Intensity expression of the GSM beams through atmospheric turbulence
k	Wave number
L	Propagation distance of the slanted path (m)
M	Beam numbers
v_g	Ground wind speed (km/h)
V	Wind speed along the vertical path (km/h)
w_0	Original beam waist width (m)
$W^{(0)}$	Cross-spectral density function of the individual beam
x_d	Distance (m)
z	Propagation distance (m)

Greek symbols

θ_{sp}	Angular spread (Rad)
λ	Wavelength (nm)

ξ	Zenith angle (Rad)
ρ_0	Spatial coherence radius of a spherical wave
σ_0	Original correlation length (m)
ω	Frequency (Hz)

REFERENCES

- [1] Fante R. VI wave propagation in random media: A systems approach. *Progress in Optics* **6** (1985), 341–398.
- [2] Strohbehn J. *Laser Beam Propagation in the Atmosphere*. Berlin: Springer Verlag. 1978.
- [3] Ionel L. Spatio-temporal analysis of the distorted chirped pulse amplification laser beam in focus. *Optoelectronics and Advanced Materials - Rapid Communications* **7**(7–8) (2013), 481–484.
- [4] Baykal Y. and Altay S. Propagation characteristics of higher-order annular Gaussian beams in atmospheric turbulence. *Optics Communications* **264**(1) (2006), 25–34.
- [5] Andrews L. and Phillips R. *Laser Beam Propagation Through Random Media*. Bellingham: SPIE Press. 1998.
- [6] Zhu S., Cai Y. and Korotkova O. Propagation factor of a stochastic electromagnetic Gaussian Schell-model beam. *Optics Express* **18**(12) (2010), 12587–12598.
- [7] Wang J.Y. Phase-compensated optical beam propagation through atmospheric turbulence. *Applied Optics* **17**(16) (1978), 2580–2590.
- [8] Fridelance P. Influence of atmospheric turbulence on the uplink propagation in an optical time transfer. *Applied Optics* **36**(24) (1997), 5969–5975.
- [9] Raphael Z. Turbulence effects on high energy laser beam propagation in the atmosphere. *Applied Optics* **29**(21) (1990), 3088–3095.
- [10] Rui Z.R. Statistics of the fractal structure and phase singularity of a plane light wave propagation in atmospheric turbulence. *Applied Optics* **47**(2) (2008), 269–276.
- [11] Tyler G.A. and Boyd R.W. Influence of atmospheric turbulence on the propagation of quantum states of light using plane-wave encoding. *Optics Letters* **34**(2) (2009), 142.
- [12] Zhao L.C., Quan Q.M., Li F.H., Li D.Y., Liu Y.G., Jin L. and Xuan L. Correction of horizontal turbulence with nematic liquid crystal wavefront corrector. *Optics Express* **16**(10) (2008), 7006–7013.
- [13] Mu Q-Q., Cao Z-L., Li D-Y., Hu L-F. and Xuan L. Open-loop correction of horizontal turbulence: system design and result. *Applied Optics* **47**(32) (2008), 4297–4301.
- [14] Yuan Y., Cai Y., Eyyuboğlu H.T. and Baykal Y. Average intensity and spreading of an elegant Hermite–Gaussian beam in turbulent atmosphere. *Optics Express* **17**(13) (2009), 11130–11139.
- [15] Ji X-L., Zhang E. and Lü B.D. Superimposed partially coherent beams propagating through atmospheric turbulence. *Journal of the Optical Society of America B: Optical Physics* **25**(5) (2008), 825–833.
- [16] Charnotskii M. Beam scintillations for ground-to-space propagation. Part I: Path integrals and analytic techniques. *Journal of the Optical Society of America A: Optics, Image Science and Vision* **27**(10) (2010), 2169–2179.
- [17] Shirai T., Dogariu A. and Wolf E. Mode analysis of spreading of partially coherent beams propagating through atmospheric turbulence. *Journal of the Optical Society of America A* **20**(6) (2003), 1094–1102.
- [18] Li X. and Ji X. Angular spread and directionality of the Hermite-Gaussian array beam propagating through atmospheric turbulence. *Applied Optics* **48**(22) (2009), 4338–4347.
- [19] Eyyuboğlu H.T. and Baykal Y. Average intensity and spreading of cosh-Gaussian laser beams in the turbulent atmosphere. *Applied Optics* **44**(6) (2005), 976–983.
- [20] Siegman A.E. New developments in laser resonators. *Proceedings of the SPIE* 1224 (1990), 2–14.

- [21] Yang A.L. and Zhang E.T., Ji X.L. and Lü B.D. Angular spread of partially coherent Hermite-cosh-Gaussian beams propagating through atmospheric turbulence. *Optics Express* **16**(12) (2008), 8366–8380.
- [22] Wang S.C. and Plonus M.A. Optical beam propagation for a partially coherent source in the turbulent atmosphere. *Journal of the Optical Society of America* **69**(9) (1979), 1427–1598.
- [23] ITU-R. Document 3J/31-E, On propagation data and prediction methods required for the design of space-to-earth and earth-to-space optical communication systems. *Radio Communication Study Group Meeting, Budapest*. ITU-R. 2001.